Published in final edited form as:
J Biol Chem. 2010 January 8; 285(2): 1122–1127. doi:10.1074/jbc.M109.058792.

PROLINE IS NOT UNIQUELY CAPABLE OF PROVIDING THE PIVOT POINT FOR DOMAIN SWAPPING IN 2G12, A BROADLY NEUTRALIZING ANTIBODY AGAINST HIV-1

Johannes S. Gach[1,5], **Paul G. Furtmüller**[2], **Heribert Quendler**[1], **Paul Messner**[3], **Ralf Wagner**[4], **Hermann Katinger**[1], and **Renate Kunert**[1]

[1]Department of Biotechnology, University of Natural Resources and Applied Life Sciences Vienna, 1190 Vienna, Austria

[2]Department of Chemistry, University of Natural Resources and Applied Life Sciences Vienna, 1190 Vienna, Austria

[3]Center for NanoBiotechnology, University of Natural Resources and Applied Life Sciences Vienna, 1190 Vienna, Austria

[4]Institute of Medical Microbiology and Hygiene, University Regensburg, 93053 Regensburg, Germany

[5]Department of Immunology and Microbial Science, The Scripps Research Institute, 92037 La Jolla, USA

Abstract

The human monoclonal antibody 2G12 is a member of a small group of broadly neutralizing antibodies against HIV-1. 2G12 adopts a unique V_H domain-exchanged dimeric configuration that results in an extensive multivalent binding surface and the ability to bind with high affinity to densely clustered high-mannose oligosaccharides on the “silent” face of the gp120 envelope glycoprotein. Here we further define the amino acids responsible for this extraordinary domain-swapping event in 2G12.

Several mechanisms have been proposed to be involved in three-dimensional (3D) domain swapping in proteins. These include 1) destabilization of the monomer, 2) accumulation of mutations in the dimer interface, and 3) modifications (e.g. deletions or mutations) in the hinge loop (1-3). All such modifications have been suggested to play a role in the domain-swapping capability of the broadly neutralizing anti-HIV-1 antibody 2G12 (4-7). The crystal structure of Fab 2G12 revealed a tightly packed Fab dimer created by 3D swapping of the variable heavy (V_H) domains. This uncommon assembly results in an additional antigen-binding site at the novel V_H/V_H’ interface in addition to two ‘conventional’ V_H/V_L binding sites (6,8,9). Several somatic mutations have been identified, particularly in the heavy chain, which could be responsible for promoting domain-exchange in this antibody (6). These amino acid substitutions are mostly localized to the V_H/V_H’ interface and ‘elbow’ region of 2G12. We have generated three IgG1 2G12 heavy chain mutants based on the Fab 2G12 crystal structure and tested their potential for domain swapping. We discovered that the domain-exchange enabling properties of Pro^{H113} at the elbow region of 2G12 can be emulated by other residues. Our results furthermore support a combination of up to four

Address correspondence to: Renate Kunert, Muthgasse 18, 1190 Vienna, Austria, Tel: +43136006-6595; Fax: +4313697615; renate.kunert@boku.ac.at; Johannes S. Gach, 10550 North Torrey Pines Road, 92037 La Jolla, Tel: +1(858) 784-2356; Fax. +1(858) 784-8360; jgach@scripps.edu.

Europe PMC Funders Author Manuscripts

somatic mutations at the V_H/V_H' interface and elbow region as being responsible for promoting domain-exchange in 2G12.

Experimental Procedures

Expression and purification of IgG1 2G12 mutants

The modified genes of the IgG1 2G12 mutants were codon optimized and synthesized by GeneArt (Germany) and stably transfected into protein free cultivated Chinese Hamster Ovary (CHO) dehydrofolate reductase deficient (dhfr-) suspension cells (ATCC CRL-9096) as described earlier (10). 24 hrs after transfection with PEI/DNA, selection was started with hypoxanthine/thymidine deficient medium. Stably transfected clones were propagated and purified over a protein A column. Quality control of purified IgG fractions was assessed by SDS-PAGE analysis. Final IgG concentrations were determined by OD_{280} measurement.

Circular dichroism (CD) spectrometry

CD analysis was performed on a PiStar-180 Spectrometer equipped with a thermostatic cell holder from Applied Photophysics (Leatherhead, U.K.). For recording near-UV spectra (240-340 nm) the quartz cuvette had a path length of 10 mm. Spectral bandwidth: 2 nm; step size: 1 nm; scan time: 21 min; protein concentration: 0.1 mg/ml. All CD measurements were performed in 5 mM PBS (pH 7.3) at 25°C (11). Each spectrum was automatically corrected with the baseline to remove birefringence of the cell. The instrument was flushed with nitrogen with a flow rate of 5 L min^{-1}.

Electron Microscopy (EM)

For the preparation of the 2G12 IgG samples freeze-drying and heavy metal shadowing was performed according to Kellenberger and Kistler (12). Electron micrographs of the antibody preparations were taken on a CM 12 electron microscope (Philips, Eindhoven, The Netherlands) at an acceleration voltage of 80 kV.

Papain digestion

Buffer exchanged (1 mM EDTA, 50 mM sodium phosphate buffer, pH 6.3) and concentrated (1 mg/ml) 2G12 IgG samples were mixed with activated papain solution (1 mM EDTA, 10 mM cysteine, 50 mM sodium phosphate buffer, pH 7.0) to give a final papain/antibody ratio of 4% (w/w). The resulting mixtures were incubated for 2 hrs at 37°C and stopped by adding 30 mM iodoacetamide. Subsequently, the cleaved antibody solution mix was buffer exchanged (PBS) and incubated twice with PBS pre-equilibrated protein A sepharose beads for 1 hr at room temperature (RT) under gentle agitation on a shaker. Finally the Fab containing supernatants were collected and further characterized by SDS-PAGE.

Gel electrophoresis

Each purified antibody sample (IgG and Fab) was mixed with Laemmli sample buffer (Bio-Rad), heated for 5 min at 100°C and examined by denaturing gel electrophoresis in a Bio-Rad Mini-Protean 3 Cell system. Subsequently, the 2G12 samples were visualized with SimplyBlue SafeStain (Invitrogen) by following the manufacturer's instructions.

ELISA

96-well microplates (eBioscience) were sensitized with recombinant gp160 MN (100 ng/well) over night (o/n) at 4°C. All following steps were carried out at RT. After washing the plates with TPBS (PBS containing 0.01 % Tween 20) the wells were blocked for 1 hr with 4% non-fat dry milk (NFDM) in TPBS. The 2G12 Fab samples (2 μg/ml) were serially

Europe PMC Funders Author Manuscripts

diluted in 1% NFDM/TPBS and added to the antigen-coated wells. After 1 hr, bound 2G12 Fab was detected with a peroxidase-conjugated goat anti-human IgG Fab conjugate (Sigma) diluted 1:1,000 in 1% NFDM/TPBS. Finally, bound conjugate was visualized with TMB substrate (Pierce) and measured at 450 nm.

Gel filtration

The papain-digested 2G12 Fab variants (100 μg/ml) were loaded in PBS (50 μl) onto a PBS equilibrated Superdex 75 10/30 column (GE-Healthcare). The protein was eluted in PBS at a flow rate of 0.5 ml/min and detected by UV absorbance.

Virus neutralization assay

JR-FL pseudovirus was generated as previously described (13) by co-transfection of a gp160 JR-FL envelope with the pSG3ΔEnv backbone. Pseudotyped virus was added at a 1:1 ratio to serially diluted (1:3) 2G12 variants (starting at 200 μg/ml) and incubated at 37°C, for 1 hr. TZM-bl cells were then seeded (1:1 by volume) at 1×10^4 cells/well in a final concentration of 10 μg/ml DEAE dextran. After 48 hr incubation at 37°C the cells were washed, lysed and finally developed with luciferase assay reagent according to the manufacturer's instructions (Promega). Luminescence in relative light units was measured using an Orion microplate luminometer (Berthold Detection Systems).

In solution virus capture assay

ELISA microplates were coated o/n with 2 μg/ml rabbit anti human Fab fragment in PBS at 4°C. The capture antibodies (2G12 Fab variants) were mixed with 100-fold concentrated JR-FL pseudovirus at a final antibody concentration of 5 μg/ml. The resulting antibody/virus mix was incubated at 37°C for 2 hrs and subsequently pelleted for 50 min at 16,000 x g at 4°C. In the meantime the coated plates were washed with PBS and blocked (3% NFDM) for 1 hr at RT. The resulting antibody/virus pellets were resuspended in PBS, transferred onto the ELISA plates and incubated for 1 hr at 37°C. Finally, plates were washed and overlaid with 1×10^4 TZM-bl cells in 100 μl/well. After 48 hrs the luciferase activity was measured as described above. All experiments were performed in duplicates.

Antibody modeling

The antibody models were generated with COOT (14) and PyMOL (15).

Results and Discussion

To further investigate the mechanism of domain swapping in 2G12, particularly the roles of previously highlighted residues at the V_H/V_H, dimer interface and elbow region, three IgG1 2G12 heavy chain mutants with multiple 'germline' amino acid substitutions in the VDJ region were created (Fig. 1A). An amino acid alignment of the V_H domains of these 2G12 mutants with that of wild-type 2G12 (2G12-wt) is shown in Figure 1B. In the first mutant, 2G12-JH3, the J-region of 2G12-wt was replaced by a corresponding germline region IGHJ3*01 resulting in five amino acid substitutions and one deletion (Fig. 1B). Two of these substitutions and the amino acid deletion occur in the complementarity-determining region (CDR) 3, whereas the remaining three substitutions are located in the J-region. For the second mutant, 2G12-GL, four additional germline amino acid substitutions are found in the V_H-region, including one substitution in the framework region (FR) 1, one in the CDR2, and two in the FR3. In a third construct, 2G12-3H6, the 2G12 V_H-region was completely exchanged by a different V_H-region derived from a previously described antibody (16,17) in order to verify the responsibility of the 2G12 DJ-region for domain swapping.

All modified 2G12 heavy chain genes and the corresponding 2G12-wt light chain genes (codon optimized and synthesized by GeneArt, Germany) were stably transfected into protein free cultivated Chinese Hamster Ovary dehydrofolate reductase deficient suspension cells (ATCC CRL-9096). The protein A purified IgG1 2G12 mutants exhibited similar electrophoretic characteristics to IgG 2G12-wt as revealed by SDS-PAGE (supplemental Fig. S1).

The IgG1 2G12-wt and IgG1 2G12 mutants were further analyzed by circular dichroism (CD) spectrometry. Measurements in the near UV-region (240-340 nm) are shown in Figure 2A. IgG1 2G12-JH3 exhibited an identical spectrum to IgG1 2G12-wt, indicating that the exchange of the J-region of IgG1 2G12-wt had no influence on the overall structure. Substitution of four additional amino acids in the IgG1 2G12-GL mutant was reflected by an apparent structural change. However, this difference may have derived from subtle changes in the local environment of particular aromatic residues, which are not necessarily associated with any major structural change (i.e. domain exchange). The spectrum of the third mutant, IgG1 2G12-3H6, revealed the largest difference to IgG1 2G12-wt. In this mutant, the whole V_H region was exchanged, which appeared to be accompanied by major structural changes. To further investigate potential structural differences between the IgG1 2G12-wt and the IgG1 2G12 mutants, electron microscopy (EM) was carried out. We used freeze-drying and heavy metal shadowing in order to visualize the frozen IgG samples in the electron microscope. Although the resolution of this preparation method was slightly lower compared to a previously described staining method (18), we were able to discriminate between I-shaped and Y-shaped conformations of the 2G12 samples (6,18). The IgG1 2G12-wt, IgG1 2G12-JH3, and IgG1 2G12-GL displayed a successively decreasing predominance of the I-shaped conformation (~ 90%, ~ 75%, and ~ 40%, respectively). In contrast, mutant 2G12-3H6 IgG1 existed predominantly in a Y-shaped conformation (~ 90%). Taken together, these EM results indicate qualitative structural differences between the different IgG1 2G12 samples (supplemental Fig. S2)

We next examined the binding capacities of Fab 2G12 mutants (produced by papain digestion) to recombinant gp160 MN (Fig. 2B). Relative affinities (i.e. apparent affinities determined from the antibody concentration at half-maximal binding) of Fab 2G12-JH3, Fab 2G12-GL, and Fab 2G12-3H6 compared to Fab 2G12-wt were less than 1%. These findings are in good correlation with those of Calarese et al. who discovered that most of their mutations to the primary combining site, secondary binding site, and V_H/V_H' interface resulted in a dramatic loss of binding to gp120 (6). Considering that the gp160 specificity ELISA might not represent an optimal environment for the 2G12 mutants the same samples were further analyzed for binding activity to native gp120 (i.e. in solution virus capture assay) as well as neutralization potency on JR-FL pseudovirus. In contrast to 2G12-wt, the mutants were neither able to capture free virus nor exhibited any neutralization capacity (data not shown).

Finally, the Fab 2G12 variants were examined for their ability to form 3D domain-swapped dimers. For this experiment, Fab 2G12 fractions were concentrated, visualized by SDS-PAGE (Fig 3A), and separated by gel filtration. Figure 3B shows the normalized spectrograms. Fab 2G12-wt eluted as two dominant peaks at 26.5 min and 30 min, corresponding to dimeric and monomeric forms, respectively. Fab 2G12-JH3 also eluted as two peaks at 26.5 min and 30 min. However, the proportion of dimer was significantly less than that for Fab 2G12-wt. In contrast, Fab 2G12-GL, Fab 2G12-3H6, and the Fab 3H6 control exhibited dominant peaks at 30 min indicating monomer only.

The fact that 2G12-JH3 still forms a dimer (Fig 3B) indicates that the Pro^{H113} to Ser substitution in the J-region does not prevent V_H domain-exchange. The high-resolution

crystal structure of Fab 2G12 (PDB 1OP3;(6)) revealed that Pro N, Cα, Cβ at the 'elbow', or hinge region of the domain-exchanged dimer are within van der Waals (VDW) contact of Val^{H84} Cγ2 (Fig. 4A). These hydrophobic interactions were proposed to stabilize the conformation of the hinge region in which the V_H domain pivots around Pro^{H113} to facilitate dimerization. Modeling of the Pro^{H113} to Ser substitution, as found in 2G12-JH3, by simply mutating the Pro^{H133} side chain to that of the most probable rotamer of the Ser side chain using the program COOT (14) suggests that these interactions could be conserved in the mutant (Fig. 4A). Moreover, the phi and psi angles of the modeled Ser lie within the preferred regions of the Ramachandran plot. Consequently, the conformation of the hinge as observed in the Fab 2G12 structure may be maintained in 2G12-JH3 via hydrophobic interactions between Val^{H84} and Ser^{H113} that are analogous to those between Val^{H84} and Pro^{H113}.

On the other hand, the fact that 2G12-GL does not form a dimer (Fig. 3B) could be due to one or a combination of the four additional substitutions found in this mutant over 2G12-JH3. As mentioned above, in the Fab 2G12 structure, Val^{H84} Cγ2 was observed to form several VDW interactions with $Pro^{H113'}$ at the elbow region, as well as with Val^{H111} O ((6); Fig. 4A). Modeling of the Val^{H84} to Ala substitution suggests that these interactions would be lost in 2G12-GL, and this may be enough to destabilize the hinge region and, hence, inhibit dimerization.

In regard to the Ile^{H19} to Arg substitution, the region of the V_H/V_H' interface around Ile^{H19} was revealed to be very tightly packed in the Fab 2G12 structure ((6); Fig 4B), with the hydrophobic side chain of Ile^{H19} being within VDW contact of $Ser^{H7'}$, $Gly^{H8'}$, $Ile^{H19'}$, $Leu^{H20'}$, $Ser^{H21'}$, and $Tyr^{H79'}$. The binding interactions in the V_H/V_H' interface would probably be significantly decreased by disruption of these hydrophobic contacts. Moreover, due to steric clashes, it is not possible to model any rotamers of the Arg side chain at this position using COOT without substantially affecting the location and rotamers of the surrounding side chains. The Ile^{H19} to Arg substitution may, therefore, not even be tolerated within the dimer interface.

In relation to the Phe^{H77} to Ser substitution, the aromatic side chain of Phe^{H77} was observed to be within VDW contact of $Thr^{H68'}$ and $Gln^{H81'}$ in the Fab 2G12 structure. (6) Modeling a Ser at this position suggests that these interactions would be lost in the 2G12-GL mutant.

The Arg^{H57} to Ile substitution would break a salt-bridge with $Asp^{H72'}$ observed at the V_H/V_H' dimer interface of Fab 2G12 (Fig 4C;(6)). In addition to the putative role of this salt-bridge in stabilizing the V_H/V_H' interface, it is also likely to be important for positioning of the neighboring Tyr^{H56} which, in the complex with Manα$_{1,2}$Man(6), forms pi-stacking interactions with Tyr^{L94} at the V_H/V_L interface. These interactions in turn may be important for the positioning of Gly^{L93} O which H-bonds with the terminal mannose O6 in the Manα$_{1,2}$Man containing arms of high mannose sugars. Notably, a Tyr^{H56} to Ala substitution was reported to cause a dramatic loss in affinity of 2G12 for gp120 (6). Moreover, Ser^{H54}, Thr^{H55}, and Arg^{H57} to Ala substitutions were similarly observed to lead to significantly decreased gp120 binding (6). These effects could similarly arise from changes in the conformation of the aromatic side chain of Tyr^{H56} which prevent it from forming pi-stacking interactions with Tyr^{L94}.

Consequently, the unusual domain-exchanged configuration of 2G12 could be fostered by the single or combined effects of four amino acid side chains that either help to stabilize the elbow region (H113) or the V_H/V_H' dimer interface. Moreover, a proline at H113 has been shown here to not be required for the domain swapping capability of 2G12. Rather, the

hydrophobic contacts between the residue at this position and the side chain of residue H84 appear to be predominantly responsible for stabilization of the elbow region.

The lack of domain swapping capability observed for the mutant 2G12-3H6 clearly indicates that the 2G12-wt CDR3 and J-region alone are not sufficient to promote V_H domain-exchange when the complete V_H-region of 2G12 is replaced by another antibody V_H-region. Taken together the present study shows that the I-shaped conformation of 2G12 cannot be traced back to a single amino acid mutation but rather involves a complex interplay of amino acid replacements. It remains to be further investigated at which stage these mutations occurred in the evolution of this very unique antibody.

Supplementary Material

Refer to Web version on PubMed Central for supplementary material.

Acknowledgments

We thank Zara Fulton (Department of Molecular Biology, The Scripps Research Institute, La Jolla, CA) for providing the 2G12 models and for critically reading the manuscript, M. Löschel, R. Marvan and K. Bauer for their excellent technical support. This work was funded by the EU project #019052, “HIVAB” and the Austrian Science Fund (J2845-B13).

REFERENCES

1. Liu Y, Eisenberg D. Protein Sci. 2002; 11:1285–1299. [PubMed: 12021428]
2. Bennett MJ, Sawaya MR, Eisenberg D. Structure. 2006; 14:811–824. [PubMed: 16698543]
3. Gronenborn AM. Curr Opin Struct Biol. 2009; 19:39–49. [PubMed: 19162470]
4. Trkola A, Pomales AB, Yuan H, Korber B, Maddon PJ, Allaway GP, Katinger H, Barbas CF 3rd, Burton DR, Ho DD, et al. J Virol. 1995; 69:6609–6617. [PubMed: 7474069]
5. Astronomo RD, Lee HK, Scanlan CN, Pantophlet R, Huang CY, Wilson IA, Blixt O, Dwek RA, Wong CH, Burton DR. J Virol. 2008; 82:6359–6368. [PubMed: 18434393]
6. Calarese DA, Scanlan CN, Zwick MB, Deechongkit S, Mimura Y, Kunert R, Zhu P, Wormald MR, Stanfield RL, Roux KH, Kelly JW, Rudd PM, Dwek RA, Katinger H, Burton DR, Wilson IA. Science. 2003; 300:2065–2071. [PubMed: 12829775]
7. Pantophlet R, Burton DR. Annu Rev Immunol. 2006; 24:739–769. [PubMed: 16551265]
8. Calarese DA, Lee HK, Huang CY, Best MD, Astronomo RD, Stanfield RL, Katinger H, Burton DR, Wong CH, Wilson IA. Proc Natl Acad Sci U S A. 2005; 102:13372–13377. [PubMed: 16174734]
9. Kwong PD, Wilson IA. Nat Immunol. 2009; 10:573–578. [PubMed: 19448659]
10. Reisinger H, Steinfellner W, Stern B, Katinger H, Kunert R. Appl Microbiol Biotechnol. 2008; 81:701–710. [PubMed: 18810429]
11. Marsche G, Furtmuller PG, Obinger C, Sattler W, Malle E. Cardiovasc Res. 2008; 79:187–194. [PubMed: 18296711]
12. Kellenberger E, Kistler J. W. Hoppe and R. Mason. 1979:49–79.
13. Nelson JD, Brunel FM, Jensen R, Crooks ET, Cardoso RM, Wang M, Hessell A, Wilson IA, Binley JM, Dawson PE, Burton DR, Zwick MB. J Virol. 2007; 81:4033–4043. [PubMed: 17287272]
14. Emsley P, Cowtan K. Acta Crystallogr D Biol Crystallogr. 2004; 60:2126–2132. [PubMed: 15572765]
15. DeLano WL. Curr Opin Struct Biol. 2002; 12:14–20. [PubMed: 11839484]
16. Gach JS, Maurer M, Hahn R, Gasser B, Mattanovich D, Katinger H, Kunert R. J Biotechnol. 2007; 128:735–746. [PubMed: 17270302]
17. Bryson S, Julien JP, Isenman DE, Kunert R, Katinger H, Pai EF. J Mol Biol. 2008; 382:910–919. [PubMed: 18692506]

18. Roux KH, Zhu P, Seavy M, Katinger H, Kunert R, Seamon V. Mol Immunol. 2004; 41:1001–1011. [PubMed: 15302162]
19. Kabat EA, Wu TT. J Immunol. 1991; 147:1709–1719. [PubMed: 1908882]
20. Gach JS, Quendler H, Weik R, Katinger H, Kunert R. AIDS Res Hum Retroviruses. 2007; 23:1405–1415. [PubMed: 18184084]

Europe PMC Funders Author Manuscripts

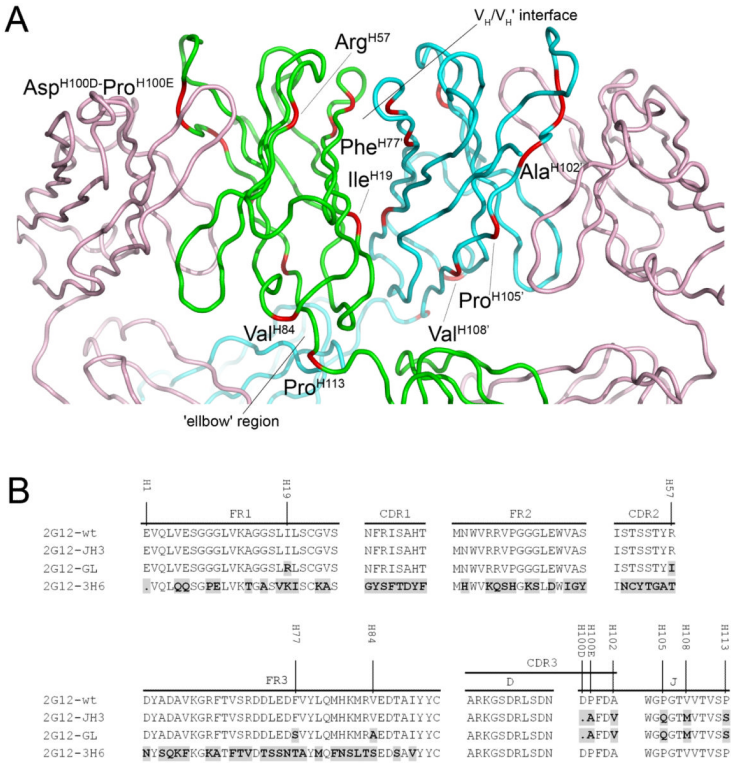

Fig 1.

2G12 Fab crystal structure *A* and amino acid alignment of the VDJ regions of 2G12 mutants compared to 2G12-wt *B*. *A* The crystal structure of Fab 2G12 with the positions of the amino acid substitutions and deletions found in 2G12-GL shown in red and labeled. The light chains of the Fab dimer are shown in pink, with the heavy chains from Fab 1 and Fab 2 shown in green and blue, respectively. The V_H/V_H' interface and the 'elbow' region are also indicated (adapted from Calarese et al. (PDB 1OP3;(6)). *B* Differences in amino acid composition of the 2G12-JH3, 2G12-GL and 2G12-3H6 mutants compared to 2G12-wt are shown in black with grey background. The amino acid numbering in *A* and *B* is based on the Kabat numbering system (19).

Europe PMC Funders Author Manuscripts

Europe PMC Funders Author Manuscripts

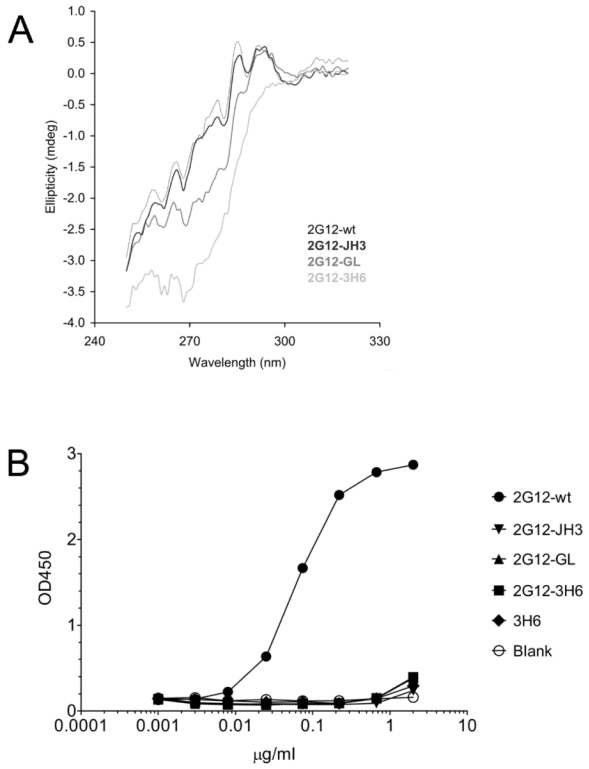

Fig 2.

2G12 IgG Circular Dichroism measurements and 2G12 Fab specificity ELISA on recombinant gp160. *A* The CD spectra in the near-UV range revealed no major structural differences between IgG1 2G12-wt, and IgG1 2G12-JH3. IgG1 2G12-GL already exhibited a slight apparent structural change. In contrast, the spectrum of IgG1 2G12-3H6 suggested major structural changes compared to IgG1 2G12-wt. *B* Only 2G12-wt Fab was able to bind to recombinant gp160 MN.

Europe PMC Funders Author Manuscripts

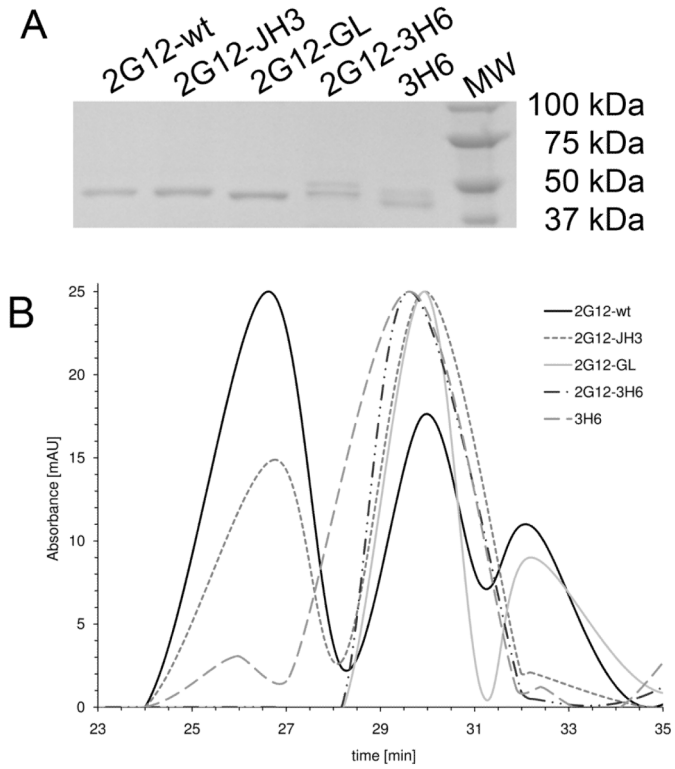

Fig 3.

SDS-PAGE of 2G12 Fab variants *A* and gel filtration *B*. *A* One band (around 53 kDa) was visible for 2G12-wt, 2G12-JH3 and 2G12-GL. An additional band (around 55 kDa) was visible for 2G12-3H6. This latter band derives from antibody 3H6, which contains an N-glycosylation site in the V_H CDR2 (20) and correlates with the two bands observed for 3H6 Fab. *B* Fab 2G12-wt eluted as both dimer and monomer. Fab 2G12-JH3 also eluted as both dimer and monomer, but with a significantly lower proportion of dimer than observed for Fab 2G12-wt. Fab 2G12-GL, Fab 2G12-3H6 and Fab 3H6 eluted as monomer only. Several protein standards with known molecular weight were also loaded onto the column to determine the size distribution of the peaks.

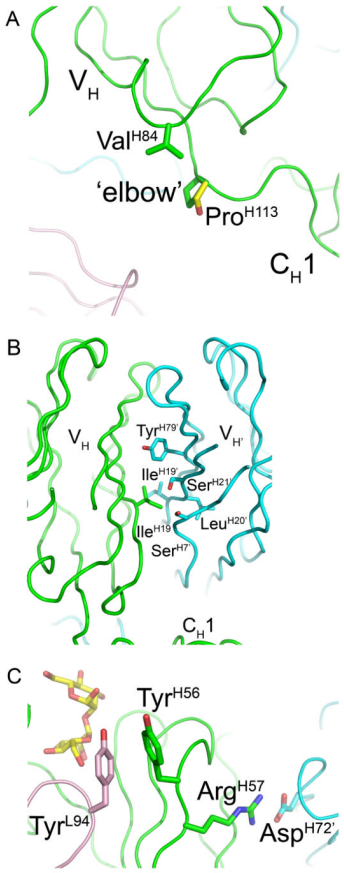

Fig 4.

Structural analysis of sequence differences between 2G12-wt, 2G12-JH3, and 2G12-GL. *A* In the high-resolution crystal structure of Fab 2G12 (PDB 1OP3; (6)), Val^{H84} Cγ2 is within VDW contact of Pro^{H113} N, Cα, Cβ, and Val^{H111} O at the elbow region of the domain-exchanged dimer. Modeling of Fab 2G12 with a Pro^{H113} to Ser substitution (Ser side chain is shown in yellow) suggests that the VDW interactions mediated by Val^{H84} Cγ2 at the elbow region in 2G12-wt could be maintained in the 2G12-JH3 mutant. *B* The hydrophobic side chain of Ile^{H19} forms extensive VDW contacts with $Ser^{H7'}$, $Gly^{H8'}$, $Ile^{H19'}$, $Leu^{H20'}$, $Ser^{H21'}$, and $Tyr^{H79'}$ in the V_H/V_H' interface of the domain-swapped dimer. *C* Arg^{H57} forms a salt-bridge with $Asp^{H72'}$ at the V_H/V_H' interface of the domain-swapped dimer. This interaction not only likely plays an important role in stabilization of the V_H/V_H' interface, but also likely plays an indirect role in 2G12 binding to clustered high-mannose oligosaccharides on gp120.